Comparative analysis of energy-level splitting of Pr^{3+} doped in $LiYF_4$ and $LiBiF_4$ crystals: a complete energy matrix calculation*

Duan Mei-Ling(段美玲)†, Kuang Xiao-Yu(邝小渝)‡,
Zhang Cai-Xia(张彩霞), and Chai Rui-Peng(柴瑞鹏)

Institute of Atomic and Molecular Physics, Sichuan University, Chengdu 610065, *China*

(Received 19 January 2010; revised manuscript received 8 February 2010)

Based on the combination of Racah's group-theoretical consideration with Slater's wavefunction, a 91×91 complete energy matrix is established in tetragonal ligand field D_{2d} for Pr^{3+} ion. Thus, the Stark energy-levels of Pr^{3+} ions doped separately in $LiYF_4$ and $LiBiF_4$ crystals are calculated, and our calculations imply that the complete energy matrix method can be used as an effective tool to calculate the energy-levels of the systems doped by rare earth ions. Besides, the influence of Pr^{3+} on energy-level splitting is investigated, and the similarities and the differences between the two doped crystals are demonstrated in detail by comparing their several pairs of curves and crystal field strength quantities. We see that the energy splitting patterns are similar and the crystal field interaction of $LiYF_4$:Pr^{3+} is stronger than that of $LiBiF_4$:Pr^{3+}.

Keywords: energy levels splitting, rare earth ions, complete energy matrix
PACS: 31.15.xp, 36.20.kd, 78.20.Bh **DOI:** 10.1088/1674-1056/20/1/013102

1. Introduction

The characteristics of compounds which are doped with rare earth (RE) elements are investigated more and more extensively these days.[1−4] $LiYF_4$ is a complex fluoride crystal that has been extensively investigated due to its attractive thermomechanical properties, wide transparence and high optical damage threshold as well as their potential applications in solid-state lasers and phosphorescence luminescent materials.[5−9] In particular, the $LiYF_4$ crystal doped with trivalent Pr^{3+} ions can be used in scintillator and wide band laser, high-definition TV and medical applications, as well as fibre communications.[10−12]

Recently the studies of $LiYF_4$ crystal doped with trivalent rare earth ions were carried out more extensively in several areas, such as, the optical satellite spectrum, the energy transition process, non-radiative decay rate, vibronic excitation transition rate and quantum upconversion.[8,9,13−20] However, the studies on $LiYF_4$:Pr^{3+} system have been scarce. Esterowitz *et al.*[21] and Schultheiss *et al.*[22] investigated the fluorescence spectrum and absorption spectrum of $LiYF_4$:Pr^{3+} crystal, measured the crystal field energy-level splitting and performed the theoretical analysis. Burdick and Richardson[23] optimised the energy parameters by using the conventional procedure for $LiYF_4$:Pr^{3+} crystal. Besides, the energy levels of Pr^{3+} ions doped in $LiYF_4$ are calculated by using a semi-empirical formula and a first principles calculation. However, the calculated data are overestimated by 20%–30%.[24] In order to provide the basis for the further study on the properties of this crystal appropriately, the energy-level splittings of the RE single electron configuration in cubic and tetragonal symmetries are discussed in this paper, and a 91×91 complete energy matrix of $4f^2$ configuration in tetragonal symmetry is constructed based on the single electron energy state information. Further, the Stark energy levels of $LiYF_4$:Pr^{3+} system are calculated and analysed systematically by diagonalising the 91×91 complete energy matrix. According to the obtained information about energy levels, some completely unknown electronic structures in crystals can be understood and the relevant optical, electric and magnetic properties can be apperceived in future.

$LiYF_4$ is related to scheelite structure, and it is a reverse scheelite-type single crystal. It belongs to $I4_1/\alpha$ space group and Y^{3+} occupies S_4 site symmetrically.[12] When RE^{3+} ions are doped into the

*Project supported by the National Natural Science Foundation of China (Grant Nos. 10774103 and 10974138).
†E-mail: meilingduan@yahoo.cn
‡E-mail: scu_kuang@163.com
© 2011 Chinese Physical Society and IOP Publishing Ltd

$LiYF_4$ crystal, they will substitute for the Y^{3+} ions and the charge compensation effect is needless to be considered due to the same trivalent ions. $LiBiF_4$ is isostructural to $LiYF_4$, so their optical, electric and magnetic properties are similar, when doped by Pr^{3+} ion. Here, we adopt several pairs of curves to make a comparison for their similarities and differences in energy-level splitting between two doped crystals in the same symmetry, and further provide the insight into the research of their optical, electric and magnetic properties.

2. Theory

2.1. Basis set

In this work, we study the energy levels of $4f^n$ configuration ion by constructing the complete energy matrixes within the ligand theory scheme by the combination of the Racah's group-theoretical consideration[25−28] with Slater's method.[29] For a $4f^n$ electron configuration, it belongs to an intermediate coupling case and basic function $|J, M_J\rangle$ is a good approximate function in order to construct the complete energy matrixes, which can be expanded into the linear combination of $|L, M_L, S, M_S\rangle$ as

$$|J, M_J\rangle = \sum_i C_i \left|L, M_L, S, M_S\right\rangle_i, \tag{1}$$

where $|L, M_L, S, M_S\rangle$ can further be expanded into the linear combination of determinantal product states as follows:

$$|L, M_L, S, M_S\rangle_j = \sum_j C_j \phi_j(m_l, m_s), \tag{2}$$

where C_i and C_j are called Clebsch–Gordon coefficients.[26]

2.2. Theoretical model

A completely effective operator Hamiltonian of $4f^n$ configuration is[30]

$$\hat{H} = \hat{H}_0 + \hat{H}_{\rm ee} + \hat{H}_{\rm so} + \sum_{i=1}^{4} \hat{H}_i({\rm corr}) + \hat{H}_{\rm CF}, \tag{3}$$

where the first three terms on the right-hand side of Eq. (3) are primarily responsible for a free ion. Their usual meanings were given by Newman and Betty.[30] The fourth term on the right-hand side of Eq. (3) is

$$\begin{aligned}\sum_{i=1}^{4} \hat{H}_i({\rm corr}) = {} & \delta(\psi, \psi')[\alpha L(L+1) \\ & + \beta G(G_2) + \gamma G(R_7)] + \sum_i t_i T^i \\ & + \sum_{i=0,2,4} m_i M^i + \sum_{i=2,4,6} p_i P^i, \end{aligned} \tag{4}$$

where the first term on the right-hand side is for interactions between configurations with the same parities, introduced by three 'Trees' parameters α, β and γ, which are associated with the eigenvalues of Casimir operators for the Lie groups R_3, G_2 and R_7,[31,32] which are

$$\begin{aligned} & G(R_3) = L(L+1), \\ & ((u_1, u_2)\,|G(G_2)|\,(u_1, u_2)) = \frac{1}{12}[u_1^2 + u_1 u_2 + u_2^2 + 5u_1 + 4u_2], \\ & ((\omega_1, \omega_2, \omega_3)\,|G(R_7)|\,(\omega_1, \omega_2, \omega_3)) = \frac{1}{10}[\omega_1(\omega_1+5) + \omega_2(\omega_2+3) + \omega_3(\omega_3+1)], \end{aligned} \tag{5}$$

here (u_1, u_2) and $(\omega_1, \omega_2, \omega_3)$ are the irreducible representations of group G_2 and R_7, respectively. They are used to specify the terms of $4f^n$ configuration ($n \leq 4$) and their definitions may be found in Ref. [31]. The usual meanings of the last three terms on the right-hand side in Eq. (4) were also explained by Newman and Betty.[30]

The fifth term on the right-hand side of Eq. (3) is for crystal field (CF) effect, which can be expressed as

$$\hat{H}_{\rm CF} = \sum_{k,q,i} B_q^k C_q^{(k)}(i), \tag{6}$$

where B_q^k parameters are related to the radial parts, and $C_q^{(k)}$ are associated with spherical parts. The rank k and projection q are limited by point group symmetry of the $4f^n$ ion site in the crystal lattice, and i runs over the electrons of the $4f^n$ configuration. Newman's superposition model (SM) of crystal field connects the geometrical information with physical information contained in lanthanide CF parameters, there

exist the following formulas:

$$B_q^k = \sum_\tau \bar{B}_k(R_\tau) g_{k,q}(\theta_\tau, \phi_\tau), \tag{7}$$

$$C_q^{(k)}(i) = \sqrt{\frac{4\pi}{2k+1}} Y_{kq}(\theta_i, \phi_i), \tag{8}$$

$$\bar{B}_k(R_\tau) = \frac{eq_\tau \langle r^k \rangle}{R_\tau^{k+1}}, \tag{9}$$

where $\bar{B}_k(R_\tau)$ are the intrinsic CF parameters, and the $g_{k,q}$ are related to the spherical harmonics functions, whose expressions may be found in Ref. [30]. According to the Hermiticity and the time-reversal invariance of the CF Hamiltonian, only the even-rank CF parameters are non-zeroes, namely, $k = 0$, 2, 4, 6 for f-electron. In Eqs. (7) and (9), τ denotes the τth ligand. In Section 3, we will discuss it in detail.

3. Analysis

3.1. Energy level splitting from T_d symmetry to $D_{2\mathrm{d}}$ symmetry for one electron

When only one unpaired f electron is contained in rare earth ions, only $\hat{H}_{\mathrm{SO}}$ and $\hat{H}_{\mathrm{CF}}$ remain in Eq. (3). This system is helpful for studying the CF and spin–orbit (SO) coupling effects. Despite an ideal system, the single electron energy state information can provide the basis for the insight into multiple electron systems. The SO coupling interaction is even larger than the CF one for rare earth f electron. For one electron system, we note that the fourteen degenerate energy levels state ^2F occurs, owing to splitting into $^2F_{7/2}$ and $^2F_{5/2}$ by the multiple of the spin–orbit coupling coefficient ζ. Of them, only one is eightfold degenerate and the others are sixfold degenerate. In the cubic T_d group symmetry, the energy levels are gradually split into the product of the three two-dimensional degenerate levels and two four-dimensional levels. When the crystal is disordered along a C_2 axis, the symmetry will be lowered from T_d to $D_{2\mathrm{d}}$ and the energy levels will be further split until the orbital degeneracy is completely removed due to the Kramer ion as suggested in Fig. 1. The numbers in the parenthesis mark the total degeneracy. The energy state information about the single electron will provide the guide for constructing a complete energy matrix of two electron systems below.

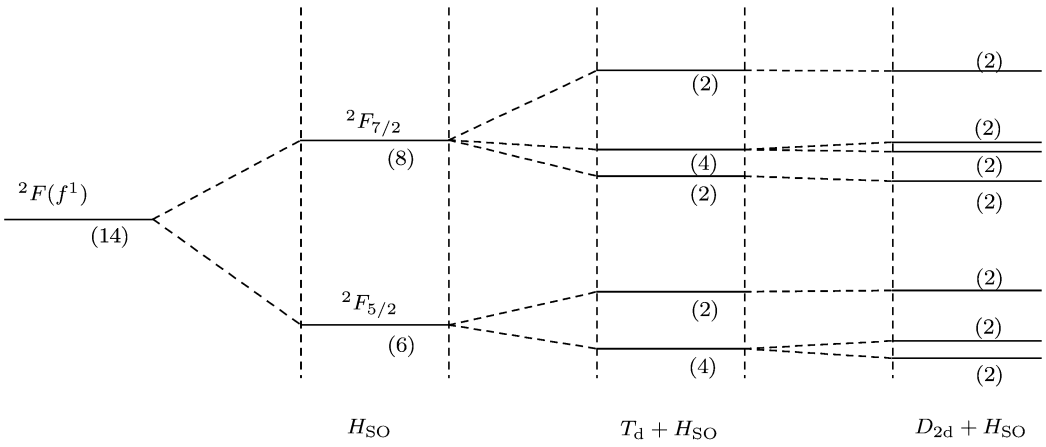


Fig. 1. Gradual energy state splitting of ^2F state from T_d symmetry to $D_{2\mathrm{d}}$ symmetry, H_{SO} denotes the spin–orbit interaction.

3.2. Energy-level structures of Pr^{3+} ions in $LiYF_4$ and $LiBiF_4$ crystals

$LiYF_4$ and $LiBiF_4$ crystals have the similar crystal structures. Both Y^{3+} and Bi^{3+} ions are surrounded by eight F^- ligands, and both the $(YF_8)^{5-}$ and the $(BiF_8)^{5-}$ entities in crystals belong to S_4 site symmetry. The distances from the four nearest F^- ligands as well as from the next-nearest four F^- ligands to the central ion are equivalent respectively. Due to the two distances are very close to each other, so we can assume the effective site symmetry to be $D_{2\mathrm{d}}$.[23] According to the Newman's superposition model and the invariability of the crystal field potential, when the symmetric operator is applied to the crystal field potential, we can obtain the Hamiltonian of $D_{2\mathrm{d}}$ symmetry as follows:

$$\hat{H}_{\rm CF} = B_0^4 C_0^{(4)} + B_4^4 (C_4^{(4)} + C_{-4}^{(4)}) + B_0^6 C_0^{(6)} + B_4^6 (C_4^{(6)} + C_{-4}^{(6)}). \quad (10)$$

Thus, a 91×91 complete energy matrix can be established according to the theory introduced in Section 2 and the information about single electron discussed in Section 3.1. Therefore, the energy-level structures of $LiYF_4$:Pr^{3+} and $LiBiF_4$:Pr^{3+} crystals can be obtained by diagonalising the complete energy matrix. The free ion and the crystal field parameters used in the calculations are listed in Table 1. The experimental energy-level data of $LiYF_4$:Pr^{3+} and $LiBiF_4$:Pr^{3+} crystals were reported[21,22] as listed in Table 2, and also shown in Table 2 are our calculation results and the differences between the calculated values and the experimental ones. We find that the relative errors are 1.5% less than the experimental values in each J-multiplet, apart from the $^3H_4$ multiplet. This indicates that our calculations are in good agreement with the measurements. The energy-level splittings also have been calculated and analysed by using the correction-crystal-field delta-function model given by Burdick and Richardson.[23] Their calculations showed that the energy levels of only the singlet multiplet manifolds were affected significantly compared with the results obtained from the standard CF model, but the triplet ones were relatively unchanged. However, our complete energy matrix calculation can simultaneously improve some energy levels of the singlet and triplet multiplet manifolds, even much closer to the experimental values. For example, for the case of $^3H_5$ multiplet, the energy of the first B irreducible representation is 2289 cm^{-1} for $LiYF_4$:Pr^{3+} crystal and that of the third E irreducible representation is 2606 cm^{-1} for $LiBiF_4$:Pr^{3+} crystal, both of them are equal to the corresponding experimental values; for the case of $^3H_6$ multiplet, the energy levels of the last three irreducible representations A, E and B are 4890 cm^{-1}, 4891 cm^{-1} and 4930 cm^{-1} for $LiYF_4$:Pr^{3+} crystal and 4873 cm^{-1}, 4887 cm^{-1} and 4925 cm^{-1} for $LiBiF_4$:Pr^{3+} crystal. They are more accurate than 4879 cm^{-1}, 4885 cm^{-1} and 4923 cm^{-1}, and also than 4857 cm^{-1}, 4871 cm^{-1} and 4906 cm^{-1} in the calculation of Burdick; so do the irreducible representations of the first B and E inter-$^3F_2$ multiplets, the E, B, A and E inter-$^3F_3$ multiplets and the first E and the nearest B inter-$^3F_4$ multiplets. For singlet multiplet manifolds, the 16802 cm^{-1} for $LiYF_4$:Pr^{3+} crystal and both 16850 cm^{-1} and 17391 cm^{-1} for $LiBiF_4$:Pr^{3+} crystal among $^1D_2$ multiplet are also close to the experimental values. All of these can imply the validity of our calculations.

Table 1. Hamiltonian parameters used in the calculation of the Stark energy-level of the two systems $LiYF_4$:Pr^{3+} and $LiBiF_4$:Pr^{3+}, all in units of cm^{-1}.

parameter	$LiYF_4$:Pr^{3+}	$LiBiF_4$:Pr^{3+}
F^2	68979	69035
F^4	50619	50716
F^6	33274	33344
α	23.0	23.0
β	–637	–641
γ	1371	1371
ζ	750	752
B_0^2	433	369
B_0^4	–1068	–862
B_4^4	1319	1367
B_0^6	–67	–37
B_4^6	1187	1040

Table 2. Measured and calculated energy values of $LiYF_4$:Pr^{3+} and $LiBiF_4$:Pr^{3+} systems, and their difference for each $^{2S+1}L_J$ multiplet is denoted with Δ_1, all in units of cm^{-1}.

term		$LiYF_4$:Pr^{3+}			$LiBiF_4$:Pr^{3+}		
	Γ	expt.	calc.	Δ_1	expt.	calc.	Δ_1
$^3H_4$	B	0	0	0	0	0	0
	E	79	87	–8	77	83	–6
	A	—	246	—	—	239	—
	A	220	246	–26	—	241	—
	E	489	499	–10	—	455	—
	A	—	509	—	—	486	—
	B	514	523	–9	—	525	—
$^3H_5$	A	2254	2269	–15	2250	2267	–17
	E	2273	2279	-6	2262	2278*	–16
	B	2289	2289	0	—	2273*	—
	A	2298	2311	–13	2294	2328	–34
	E	2341	2355	–14	2317	2341	–24
	B	2549	2580	–31	—	2573	—
	A	—	2599	—	—	2589	—
	E	—	2621	—	2607	2606	1

Table 2. (*Continued*).

term		$LiYF_4:Pr^{3+}$			$LiBiF_4:Pr^{3+}$		
	Γ	expt.	calc.	Δ_1	expt.	calc.	Δ_1
$^3H_6$	B	4313	4322	–9	4320	4341	–21
	E	4391	4419	–28	4391	4427	–36
	A	—	4427	—	—	4429	—
	B	—	4483*	—	—	4490	—
	E	4453	4482*	–29	4449	4491	-42
	A	4486	4521	-35	—	4541	—
	B	4551	4562	–9	4510	4548	–38
	A	4904	4890	14	4881	4873	8
	E	4910	4891	19	4887	4887	0
	B	4949	4930	19	4921	4925	–4
$^3F_2$	A	—	5166	—	—	5156	—
	B	5204	5229*	–25	5168	5193	-25
	E	5223	5221*	2	5192	5199	–7
	B	5348	5320	28	5307	5287	20
$^3F_3$	E	6484	6485	–1	6479	6487	–8
	B	6527	6530	–3	6515	6529	–14
	A	6591	6570	21	—	6562	—
	E	6676	6674	2	6647	6650	-3
	B	6691	6721	–30	6682	6686	–4
$^3F_4$	A	6923	6950*	-27	6902	6932	-30
	E	6946	6945*	1	6928	6935	-7
	B	6983	6983	0	7003	6972	31
	A	7105	7161	–56	—	7135	—
	B	7116	7164	–48	—	7173	—
	E	7147	7176	–29	7123	7177	–54
	A	7224	7275	–51	7189	7255	–66
$^1G_4$	A	9707	9695	12	9708	9702	6
	E	9837	9790	47	9840	9804	36
	B	9930	9910	20	—	9897	—
	B	10011	10030	–19	—	10073	—
	A	—	10138	—	—	10121	—
	E	10123	10177	–54	10105	10191	-86
	A	—	10604	—	—	10560	—
$^1D_2$	B	16746	16802	-56	16744	16806	–62
	A	16813	16819	–6	16847	16850	–3
	E	17092	17068	24	17086	17066	20
	B	17408	17384	24	17391	17391	0
$^3P_0$	A	20866	20783	83	20853	20784	69
$^1I_6$	B	—	21289	—	—	21372	—
	B	—	21290	—	—	21377	—
($^3P_1$)	E	(21412)	(21368)	(44)	(21402)	(21378)	(24)
	E	—	21542	—	—	21529	—

Table 2. (*Continued*).

term		$LiYF_4:Pr^{3+}$			$LiBiF_4:Pr^{3+}$		
	Γ	expt.	calc.	Δ_1	expt.	calc.	Δ_1
$(^3P_1)$	A	(21476)	(21514)	(–38)	(21457)	(21504)	(–47)
	A	—	21553	—	—	21540	—
	B	—	21556	—	—	21547	—
	E	—	21803	—	—	21804	—
	A	—	21940	—	—	21912	—
	A	—	22221*	—	—	22217*	—
	E	—	22219*	—	—	22215*	—
	B	—	22221	—	—	22217	—
$^3P_2$	A	22496	22554	–58	22531	22573	–42
	E	22648	22686	–38	22628	22682	-54
	B	—	22704	—	—	22696	—
	B	—	22814	—	—	22807	—
$^1S_0$	A	—	47124	—	—	47176	—

* The calculated Stark energy levels that have been reordered to corresponding energy assignments.

Besides, we note that the irreducible representations in $LiYF_4:Pr^{3+}$ and $LiBiF_4:Pr^{3+}$ crystals are similar. This reflects that their crystal structures are similar, which further leads to the identical energy level splitting patterns. We also plot several pairs of curves in order to explain this point as shown in Figs. 2(a)–2(d), where symbol Δ refers to the energy interval between two adjacent irreducible representations of the inter-multiplet and the abscissa represents the number of the energy intervals. Figures 2(a) and 2(b) show the comparisons of triplet states $^3H_6$ and $^3F_4$ between the two crystals respectively, $^3H_6$ and $^3F_4$ states characterized by more energy intervals than the other triplet states can be perceived as a representative and can produce a good persuasiveness. Correspondingly, Figs. 2(c) and 2(d) exhibit the comparisons of single states $^1G_4$ and $^1I_6$ between the two crystals respectively. We see that the peaks of curves for $LiYF_4:Pr^{3+}$ crystal almost keep accordant with those for $LiBiF_4:Pr^{3+}$ crystal. This also indicates the similarities in energy level splitting scheme and crystal field interaction of $4f^2$ configuration ion for these two crystals.

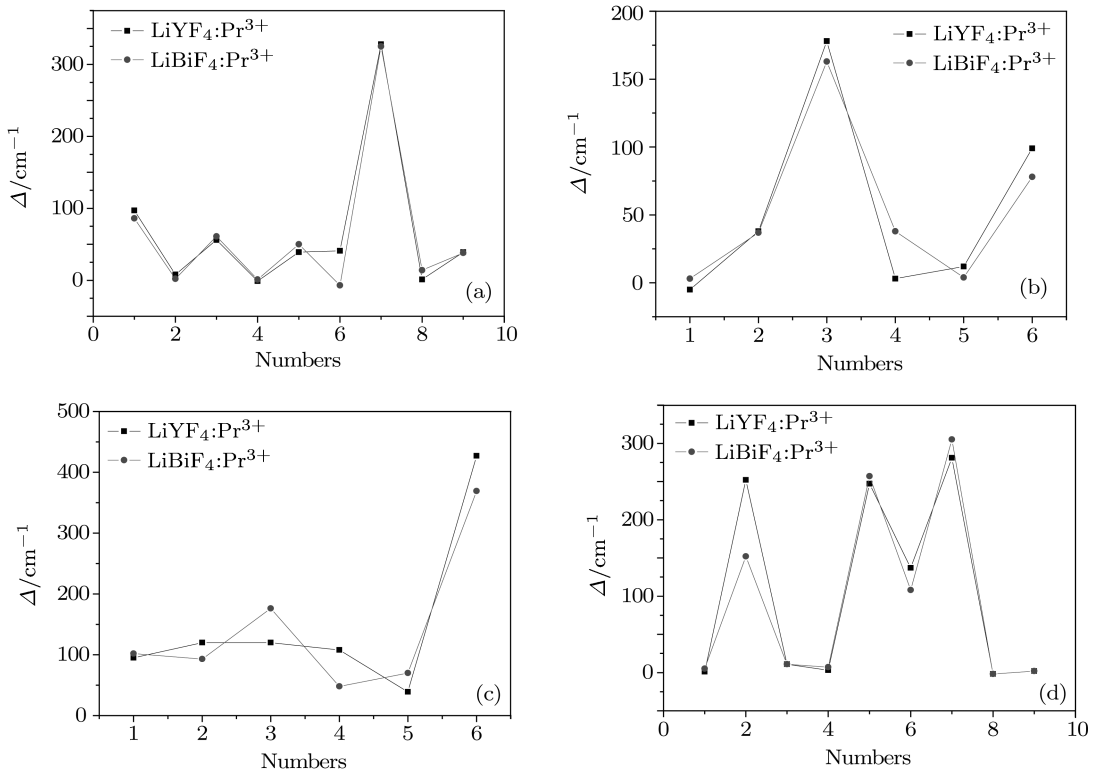


Fig. 2. Curves for comparisons of crystal field strength between crystals $LiYF_4:Pr^{3+}$ and $LiBiF_4:Pr^{3+}$ for (a) $^3H_6$ multiplet, (b) $^3F_4$ multiplet, (c) $^1G_4$ multiplet and (d) $^1I_6$ multiplet.

3.3. Comparison of crystal field strength between $LiYF_4$:Pr^{3+} and $LiBiF_4$:Pr^{3+}

From the above, we know that the crystal field splitting patterns are identical for $LiYF_4$:Pr^{3+} and $LiBiF_4$:Pr^{3+} crystals, nevertheless, we also note their differences. Compared with $LiYF_4$:Pr^{3+} crystal, the $LiBiF_4$:Pr^{3+} crystal has the energy levels that are separated slightly weakly. Visually, the points describing the $LiBiF_4$:Pr^{3+} are situated almost at the lower positions relative to the $LiYF_4$:Pr^{3+} as shown in Fig. 2. In this section, the crystal field strength quantities $S^k_{\rm cf}$ and $S_{\rm cf}$ are introduced to reveal their differences quantitatively, and they are expressed as

$$S^k_{\rm cf} = \left\{ \frac{1}{2k+1} \left[(B^k_0)^2 + 2 \sum_{q>0} \left| B^k_q \right|^2 \right] \right\}^{1/2},$$

$$S_{\rm cf} = \left[\frac{1}{3} \sum_k (S^k_{\rm cf})^2 \right]^{1/2}. \quad (11)$$

From the results listed in Table 3 it follows that the values of $S^k_{\rm cf}$ (k = 2, 4, 6) and $S_{\rm cf}$ for $LiBiF_4$:Pr^{3+} system are smaller than those for $LiYF_4$:Pr^{3+} system, which shows that the influence of Pr^{3+} ion on $LiBiF_4$:Pr^{3+} crystal is slightly weaker than that on $LiYF_4$:Pr^{3+} crystal. It may be due to the bigger ionic radius of Bi^{3+} (0.96 Å) (1 Å=0.1 nm) than that of Y^{3+} (0.89 Å), which results in the smaller interaction between the central ions and ligand ions in $LiBiF_4$:Pr^{3+} crystal. We conclude that the influence degree of the dopant ion on the energy level of the host crystal is related to the ionic radius of the replaced ion in the host crystal.

Table 3. Crystal field strength quantities of the two systems, all in units of cm^{-1}.

parameters	$S^2_{\rm cf}$	$S^4_{\rm cf}$	$S^6_{\rm cf}$	$S_{\rm cf}$
$LiYF_4$:Pr^{3+}	194	716	466	506
$LiBiF_4$:Pr^{3+}	165	706	408	480

4. Conclusions

The analysis of energy state for one unpaired f electron in D_{2d} symmetry provides a guide for establishing the complete energy matrix of multiple electrons systems. Based on an established 91×91 complete energy matrix of $4f^2$ configuration ions in tetragonal ligand field, we calculate the Stark energy levels of $LiYF_4$:Pr^{3+} and $LiBiF_4$:Pr^{3+} crystals. The results show that the calculated values are in good agreement with the experimental ones and our calculations can simultaneously improve the energy levels of the singlet and the triplet multiplet manifolds compared with the calculations by using the correction-crystal-field delta-function model. This implies that the complete energy matrix method is an effective and reasonable method of calculating and analysing the energy levels of $4f^2$ configuration ion doped in crystals. In addition, we note that the influence of Pr^{3+} ion on energy level splitting of $LiYF_4$ is slightly stronger than that of $LiBiF_4$ as shown by the comparison of several pairs of curves, and this can also be verified by several crystal field strength quantities. Furthermore, we can draw a conclusion that the influence degree of dopant ion on energy level of the host crystal is dependent on the ionic radius of the replaced ion in the host crystal.

References

[1] Liu F, Zhang J H, Lü S Z and Wang X J 2006 *Acta Phys. Sin.* **55** 6020 (in Chinese)

[2] Li P L, Wang Z J, Wang Y, Yang Z P, Guo Q L, Li X, Yang Y M and Fu G S 2009 *Acta Phys. Sin.* **58** 5831 (in Chinese)

[3] Ma C G, Jiang S, Duan C K, Yin M and Xia S D 2009 *Chin. Phys.* B **18** 1961

[4] Yang H G, Dai Z W and Zu N N 2007 *Chin. Phys.* **16** 1650

[5] Wells J P R, Sugiyama A, Han T P J and Gallagher H G 2000 *J. Lumin.* **87–89** 1029

[6] Rogin P, Huber G and Hulliger J 1999 *J. Cryst. Growth* **198/199** 564

[7] Dong H N, Zheng W C, Wu S Y and Tang S 2004 *Spectrochim. Acta* A **60** 489

[8] Combes C M, Dorenbos P, van Eijk C W E, Pedrini C, Den Hartog H W, Gesland J Y and Rodnyi P A 1997 *J. Lumin.* **71** 65

[9] Yin J G, Zhang Q R, Liu T Y, Guo X F, Song M, Wang X and Zhang H Y 2009 *Physica* B **404** 1053

[10] Rogin P and Hulliger J 1997 *J. Cryst. Growth* **179** 551

[11] Khiari S, Velazquez M, Moncorgé R, Doualan J L, Camy P, Ferrier A and Diaf M 2008 *J. Alloys Compd.* **451** 128

[12] Yin J G, Zhang Q R, Liu T Y, Guo X F, Song M, Wang X and Zhang H Y 2009 *Nuclear Instruments and Methods in Physics Research* B **267** 74

[13] Malkin B Z, Vanyunin M V, Graf M J, Lago J, Borsa F, Lascialfari A, Tkachuk A M and Barbara B 2008 *Eur. Phys. J.* B **66** 155

[14] Braud A, Girard S, Doualan J L, Thuau M and Moncorgé R 2000-II *Phys. Rev.* B **61** 5280

[15] Wells J P R, Yamaga M, Han T P J, Gallagher H G and Honda M 1999-II *Phys. Rev.* B **60** 3849

[16] Donegá C de M, Meijerink A and Blasee G 1995 *J. Phys. Chem. Solids* **56** 673
[17] Tsuboi T, Murayama H and Shimamura K 2006 *J. Alloys Compd.* **408–412** 776
[18] Tigreat P Y, Doualan J L, Budasca C and Moncorge R 2001 *J. Lumin* **94–95** 23
[19] Louis M, Hubert S, Simoni E and Gesland J Y 1996 *Opt. Mat.* **6** 121
[20] Kück S and SokÓlska I 2000 *Chem. Phys. Lett.* **325** 257
[21] Esterowitz L, Bartoli F J, Allen R E, Wortman D E, Morrison C A and Leavitt R P 1979 *Phys. Rev.* B **19** 6442
[22] Schultheiss E, Scharmann A and Schwabe D 1987 *Phys. Stat. Sol.* B **140** 173
[23] Burdick G W and Richardson F S 1998 *Chem. Phys.* **228** 81
[24] Ogasawara K, Watanabe S, Toyoshima H, Ishii T, Brik M G, Ikeno H and Tanaka I 2005 *J. Solid State Chem.* **178** 412
[25] Racah G 1942 *Phys. Rev.* **61** 186
[26] Racah G 1942 *Phys. Rev.* **62** 438
[27] Racah G 1943 *Phys. Rev.* **63** 367
[28] Racah G 1949 *Phys. Rev.* **76** 1352
[29] Slater J C 1960 *Quantum Theory of Atomic Structure*, Vol. 2 (USA: Mcgraw-Hill Book Company, Inc.)
[30] Newman D J and Betty Ng 2000 *Crystal Field Handbook* (UK: Cambridge University Press)
[31] Budd B R 1963 *Operator Techniques in Atomic Spectroscopy* (New York: Mcgraw-Hill Book Company, Inc.)
[32] Rajnak K and Wybourne B G 1963 *Phys. Rev.* **132** 280